SNA + MC 2013, 02404 (2014)
DOI: 10.1051/snamc/201402404

Sensitivity Analysis for Activation Problems

Wayne Arter[1] and J. Guy Morgan[2]

[1] *UK Atomic Energy Authority, Culham Science Centre, Abingdon OX14 3DB, United Kingdom*
[2] *Culham Electromagnetics Ltd, Culham Science Centre, Abingdon OX14 3DB, United Kingdom*

A study has been made as to how to develop further the techniques for sensitivity analysis used by FISPACT-II. FISPACT-II is a software suite for the analysis of nuclear activation and transmutation problems, developed for all nuclear applications. The software already permits sensitivity analysis to be performed by Monte Carlo sampling, and a faster uncertainty analysis is made possible by a powerful graph-based approach which generates a reduced set of nuclides on pathways leading to significant contributions to radiological quantities. The peculiar aspects of the sensitivity analysis problem for activation are the large number, typically thousands, of rate equation parameters (decay rates and reaction cross-sections) which all have some degree of associated error, and the fact that activity as a function of time varies as a sum of exponentials, so appears discontinuous as rate parameters are varied unless the sampling frequency is impractically fast. Nevertheless, Monte Carlo sampling is a generic approach and it is therefore conceivable that techniques more targeted to the activation problem might be beneficial. Moreover, recent theoretical developments have highlighted the importance of a two-stage approach to mathematically similar problems, where in the first stage, information is collected about the global behaviour of the problem, such as the identification of the rate parameters which cause the greatest variation in dose or nuclear activity, before a second stage examines a problem with its scope restricted by the information from the first. In the second stage, for example, Quasi-Monte Carlo sampling may be used in a restricted parameter space. The current work concentrates on the first stage and consists of a review of possible techniques with a detailed examination of the most promising pathways reduction approach, examined directly using FISPACT-II. All the evidence obtained demonstrates the strong potential of this approach.

KEYWORDS: Activation, Sensitivity Analysis, Screening design, FISPACT-II.

I. Introduction

FISPACT-II[(1)] is a modern software suite for the analysis of nuclear activation problems, originally developed for nuclear fusion applications, but now also extensively used in nuclear fission and astrophysics problems. Indeed, the ongoing development of the software takes into account the needs of all the likely application areas. For a typical activation problem, thousands of rate equation parameters, corresponding to nuclear decay rates and reaction cross-sections, may influence the activity throughout its history. All of these parameters are subject to significant uncertainty due to experimental error in their measurement or theoretical approximations made in their calculation. Since the dose rate, a weighted sum of separate nuclide activities, is safety critical, it is important to be able to estimate how uncertainties in the parameters contribute to the calculation of activity.

For problems with a small number of parameters, the mean and standard deviation dose or nclear activity may be calculated by sampling each parameter at a number of points uniformly distributed in its distribution then using each set of sample values to perform a FISPACT-II calculation. However, this approach, known as factorial sampling, suffers from the curse of dimensionality in that the total number of samples required increases exponentially with number of parameters K. This helps explain why the Monte Carlo technique is popular. Sample points are selected at random throughout the K-dimensional parameter space to avoid the exponential growth. Unfortunately, the convergence of the mean of the samples is slow, proportional to $1/\sqrt{N_s}$, where N_s is the number of sample points.[(2)]

Quasi-Monte Carlo (QMC)[(3)] sampling may offer an acceptable cost-quality compromise in that it offers a faster rate of convergence, approaching $1/N_s$. When it is realized that QMC is, despite its name, basically a deterministic approach, it will be understood that it is difficult to avoid spurious correlations among the sample points as K increases. These correlations may destroy the good convergence properties of QMC once K gets up to a value of 20 to 50, even using the latest techniques.[(4)] Similar remarks appear to apply to importance sampling based on the Markov chain Monte Carlo methodology, or integration via adaptive Monte Carlo. Hence, activation sensitivity analysis often involves a first 'screening' stage that seeks to reduce the size of the parameter space to be examined.

This issue is already addressed from a practical standpoint in FISPACT-II by selecting a reduced set of nuclides on reaction and decay pathways that lead from an initial inventory to target nuclides that give dominant contributions to the radiological quantities of interest. This approach suppresses the combinatorial explosion sufficiently for useful calculations to be performed. An advantage of this method is that it can accommodate arbitrary sequences of irradiation and cooling steps.[(5)]

II. Screening Design

1. General

Historically, sensitivity analysis has often been conducted in two stages, with a first 'screening design' step, to try to identify those parameters which cause the greatest variation in computed dose or activity, followed by a detailed investigation of the results of varying the indicated parameters.[6] A number of different techniques were developed for this, of which the commonest is 'One-at-a-Time' (OAT) where one parameter is varied while all the others are held fixed at some central value. This only requires $N_s = O(K)$ samples, but obviously is very limited in its examination of sample space and does not yield activity values immediately suitable for calculating the mean. The other popular strategy is non-deterministic, namely Morris, which involves the construction of random walks designed so that they take one step in each coordinate direction in sample space. Very recently,[7] a non-deterministic version of OAT has been proposed, which selects central points at random in parameter space. This has the advantage that data are generated which can be easily reused to calculate mean and variance in the second stage.

Nonetheless, all these methods have their disadvantages, exemplified by the need to choose a step-size for the parameter variation. If too small, large important regions of parameter space may be ignored. If the step is too large, important local variation may be missed, because the activity does not necessarily have monotonic dependence on a parameter.

2. Activation-Specific Screening Designs

2.1. Eigenvalue Analysis

An interesting technique is enabled simply by the linearity of the rate equations with respect to nuclide number, assuming a fixed irradiation rate, viz.

$$\frac{dN}{dt} = \mathsf{A}N \tag{1}$$

where A is the matrix of parameters and N is the vector of nuclide numbers, (the nuclear inventory). Mathematical theory indicates that the solution is given as a sum of eigenvectors $\mathbf{e}_i$ of A, where each $\mathbf{e}_i$ is associated with an eigenvalue λ_i of A. This solution reveals the specific sensitivities of the activation problem, since activity Q is a weighted sum of the numbers of nuclides present at a given time.

In particular, if Q is required at time t_0, its value can be sensitive only to those eigenvectors for which λ_i satisfies $\lambda_i \approx 1/t_0$. For, if λ_i is either much smaller or larger, then the properties of the decaying exponential imply that Q is effectively constant as a function of λ_i or zero. Since eigenvalue sensitivity analysis is a well-developed mathematical technique, it may be used to discover which entries in A most affect the 'sensitive' eigenvalues. The algorithms for eigenvalue sensitivity analysis have a complexity of $O(M^3)$ where M is the size of the matrix A, but given the Gigaflop speed of modern PCs, it may be estimated that even for $M \approx 4000$, an analysis on a desktop machine may be completed in under an hour.

There seem unfortunately to be severe difficulties with this approach. The biggest appears to be the huge range of nuclear decay rates in the EASY databases. To take as an example, EAF 2010, it contains data for 7 nuclides with decay rates $>\approx 10^{21}$ s^{-1}, together with Uranium nuclides with half-lives $t_{1/2}$ of the order of 10^{10} yr, i.e. $\lambda \approx 10^{-17}$ s^{-1}, and of course 228 stable nuclides with decay rate 0. The error estimates for standard eigenvalue algorithms imply that a precision significantly greater than $21 + 17 = 38$ decimal digits is required, compared to the 15 to 16 digits available in double precision.

Another potential difficulty is that many decay rates are only approximately known, so that for example some tens of nuclides in the database have $t_{1/2}$ given as 1 ms, meaning that a corresponding number of non-zero eigenvalues may be very closely spaced. It is apparent that the mathematical eigenvalue calculation requires research in its own right.

One way of making the eigenvalue problem tractable is to reduce the size of the rate matrix A, an idea which leads naturally onto the work of the next section.

2.2. Pathways Reduction

A possible screening method specific to the activation problem could use information gained from the existing pathways analysis. The new pathways reduction method was designed and implemented by the developers of Fispact-II[5,8]. For present purposes, it is sufficient to explain that the dominant nuclides at a specified time are identified by simple examination of the inventory. 'Dominant' nuclides are those which produce either the biggest dose rates or the largest activities. Graph theoretic techniques are then used to identify the most important nuclear pathways leading from the nuclides in the original inventory to the dominant nuclides. Nuclides on these pathways are listed, and only these nuclides with the obvious addition of the initial and dominant nuclides, are used to define a new model problem with typically a much smaller size of rate matrix A. Reactions and decays resulting in products not on the pathways allocate their products to an inert 'sink' nuclide which produces no activity or radiological dose.

The key question is: how much is lost by this reduction? Almost certainly there will be a reduction in total Q, because there will be fewer nuclides present in the final inventory. However, this reduction may be easily estimated by comparison with the full calculation. For sensitivity analysis, the important issue concerns what happens to the distribution of final inventories as reaction coefficients are varied within their range of uncertainty. The easiest way to examine this is by a Monte Carlo analysis as implemented in Fispact-II. A series N_s of inventory calculations is performed with the set of I independent variables $\{X_i^s;\ i = 1, \ldots, I;\ s = 1, \ldots, N_s\}$ chosen from distributions with means $\langle X_i \rangle$ and standard deviations $\langle \Delta X_i \rangle$. The default distribution studied is log-normal. These runs produce a set of J dependent variables $\{Y_j^s;\ j = 1, \ldots, J;\ s = 1, \ldots, N_s\}$. In the present context, the independent variables are cross-sections and their uncertainties, because as presently implemented, examination of decay constants and their uncertainties is not possible. The dependent variables are the numbers of atoms of nuclides j or some related radiological quantity such as dose

or activity. The user specifies a number N_x of Monte Carlo samples to be taken for each cross-section, hence $N_s = N_x I$.

The code performs an initial, 'base' calculation with full output, then repeats N_s times the sequence of steps with different sets $\{X_i^s\}$. Sensitivity calculations provide both uncertainty and sensitivity output, as described in ref [1, A.11]. The uncertainty output, of means $\bar{X}_i$ and $\bar{Y}_j$ and standard deviations ΔX_i and ΔY_j, is of most interest in the present context, although the sensitivity estimates (Pearson product-moment correlation coefficients) might be of at least equal value in subsequent research into model reduction.

$$\bar{X}_i = \frac{1}{N_s}\sum_{s=1}^{N_s} X_i^s \quad (2)$$

$$\Delta X_i = \sqrt{\frac{1}{N_s - 1}\sum_{s=1}^{N_s}[(X_i^s)^2 - \bar{X}_i^2]} \quad (3)$$

$$\bar{Y}_j = \frac{1}{N_s}\sum_{s=1}^{N_s} Y_j^s \quad (4)$$

$$\Delta Y_j = \sqrt{\frac{1}{N_s - 1}\sum_{s=1}^{N_s}[(Y_j^s)^2 - \bar{Y}_j^2]} \quad (5)$$

Attention will focus on the relative standard deviations $\sigma_{rstd} = \Delta Y_j / \bar{Y}_j$ as detailed measures of the distributions of inventories produced by the Monte Carlo sampling.

In addition to writing tables of means, standard deviations and correlation coefficients, FISPACT-II writes the raw data $\{X_i^s,\ Y_j^s;\ i = 1, \ldots, I;\ j = 1, \ldots, J;\ s = 1, \ldots, N_s\}$ to a separate '`sens`' file for post-processing. These `sens` data are the basis for subsequent comparisons between full and reduced (pathways) analyses.

III. Monte Carlo Analysis

1. Details of Computations

FISPACT-II has the capability to treat a vast range of activation problems, and over a hundred standard tests are supplied with the software, although not all involve different nuclides. To capture as much of this range of possible for a reasonable effort, the seven nuclide mixtures listed in Table 1 have been composed. As indicated, most of the mixtures consisted of 1 kg of material subject to a neutron flux of 10^{15} cm^{-2}s^{-1}, for a year, without any cooling period. However, to produce a fission problem, an existing test case with a smaller sample, flux and irradiation time was used. Further, to compare with experimental data for Y_2O_3, a much smaller sample, flux and irradiation time was used.

The mixtures are used in eight test cases, with the Alloy case extended to including a cooling phase. (Cooling is expected to simplify greatly sensitivity analsysis, since it tends to reduce the number of significant nuclides in the inventory.) Each test case is run using the full TENDL 2012 database with pathways analysis to identify the dominant nuclides and important reactions, total numbers of which are listed in Table 2. The sole exception is the YO2 case where a single nuclide, ^{86}Rb is selected for study. This represents a particularly searching examination of pathways reduction, as ^{86}Rb is a very small contributor to the the inventory. Monte Carlo solution of the full problem, studying the allowed variations in the important reaction rates, is then performed in the sequence of increasing sample size per reaction, $N_x = 10,\ 40,\ 160,\ \ldots$ up to the maximum value specified in the table. For each mixture, provided the same machine is used, the cost of a FISPACT-II calculation scales linearly with N_s to a very good approximation. (Some of the computation times listed may not be strictly comparable, because the Linux cluster used in the investigation is heterogeneous.)

The full (F) calculations produce information that is used to define reduced pathways (R) calculations. For each test case, an initial FISPACT-II (R) calculation defines fluxes and rate data needed for a sequence of Monte Carlo solutions analogous to that described in the preceding paragraph.

2. Test Case Comparisons

Each test case has been subject to a detailed programme of investigation. First, for each of the F and R cases separately, convergence of the distribution of activity with respect to N_s has been demonstrated by plotting histograms. Next, for the highest (and invariably converged) sampling rate, the two distributions for F and R are compared and found to agree to graphical accuracy. More quantitatively, gaussian and log-normal distribution functions are fitted to the histograms (using the gnuplot *fit* function[9]). Results of this procedure appear in Tables 3 and 4. Lastly, and comprising the most searching examination, the relative standard deviations for the distribution of each nuclide separately are compared graphically.

The degree of accuracy to which the graphical comparisons are accurate can of course be gauged only by looking at the plots reproduced below. However, from 8 test cases, there are simply too many graphs to reproduce all of them. The selection procedure adopted is to show all the graphs for one mixture, and a second graph of each type for a different mixture. The second graphs are of the mixtures arranged in alphabetical order, except that the Fiss and WMix test cases appear after the Y2O3 case.

The fitting of non-Gaussian distributions to the data in Table 4 is questionable in many cases, indeed it is apparently impossible in some, because it is expected that the estimated mean μ should be less for the R cases than for the F ones. Note that the expected ordering is invariably found for Gaussian fitting, even in the Fe test problem, where the standard deviation σ is smaller than the difference between the F and R cases. (The two histograms of activity distributions can be reconciled by the simple expedient of offsetting the F case by the μ difference.) Nonetheless, the agreement found between the fitting parameters for equivalent F and R cases, as indicated by the formal % error statistics is impressive.

Detailed examination of the relative standard deviation statistic σ_{rstd} shows that the F and R estimates usually agree to within two significant figures, although occasionally only to within one and the smaller values of σ_j ($< 10^{-3}$) are capable of showing even poorer agreement. Agreement only to one

Table 1: Test cases. Apart from the Fiss mixture, each consists of numbers of atoms of the listed elements with their natural abundances of nuclides, given as percentages of the whole.

Test Label	Constituents of Mixture	Sample Mass	Irradiation Period	Cooling Period	Neutron flux $cm^{-2}s^{-1}$
Alloy	Fe 40.0 : Ni 20.0 : Cr 20.0 : Mn 20.0	1 kg	1 yr	0	10^{15}
Alloy+c	Fe 40.0 : Ni 20.0 : Cr 20.0 : Mn 20.0	1 kg	1 yr	1 yr	10^{15}
Fe	Fe	1 kg	2.5 yr	0	10^{15}
Fiss	U235 3.7 : U238 96.3	8.7 g	3 mo	0	2.59032×10^{14}
LiMix	Li 40.0 : Be 30.0 : O 30.0	1 kg	1 yr	0	10^{15}
WMix	W 20.0 : Re 20.0 : Ir 20.0 : Bi 20.0 : Pb 20.0	1 kg	1 yr	0	10^{15}
Y2O3/YO2	Y 78.74 : O 21.26	1 g	300 s	0	1.116×10^{10}

Table 2: Test cases statistics. The entries in the columns labelled 'Full' and 'Pathways Reduced' are the numbers of dominant nuclides. (See text for detailed discussion of the computation times.)

Test Label	I, Reactions Examined	Full	Pathways Reduced	Matrix A Size	Max. N_x, Samples per Reaction	N_s, Total Sample	Reduced cpu (s)	Full cpu (s)
Alloy	76	23	23	53	640	48 640	82.053	44 136
Alloy+c	50	13	13		640	32 000	56.494	38 623
Fe	26	20	13	23	640	16 640	9.6355	13 995
Fiss	1	47	47		2 560	2 560	33.143	10 143
LiMix	17	9	9	23	640	10 880	4.0664	8 011
WMix	71	29	29	69	640	45 440	96.947	47 019
Y2O3	12	11	11	16	2 560	30 720	4.7893	13 526
YO2	2	1	1		10 240	20 480	2.1057	8 944

significant figure is found for the YO2 test case, but given the tiny contribution of ^{86}Rb to the total activity, this is probably reasonable and consistent with the good quantitative agreement between the larger F and R σ_{rstd} values found in the other test cases.

IV. Summary

Work has been performed to examine the suitability of an activation-specific screening design method for use in the FISPACT-II suite. A large amount of evidence, from the Monte Carlo sampling of 8 different test problems, has been gathered that pathways reduction is a most useful technique.

The distributions of activity per sample obtained by pathways reduced calculations have been examined, and compared with those produced by full FISPACT-II calculations. Numerical parameters for Gaussian and log-normal distributions fitted to the computed activities agree to at least 2 significant figures, often 3, as shown in Tables 3 and 4. Histograms of the distributions in Section III show detailed agreement. Very significantly, (relative) standard deviations of distributions of separate nuclides have been shown to vary little between reduced and full calculations.

In three of the test cases, the number of significant reactions K was reduced to below 50 where more efficient sampling techniques could be considered immediately. In all except the fission problem, $K < 100$ may be estimated, and for further analysis of these cases it will help that, as indicated in Table 2,

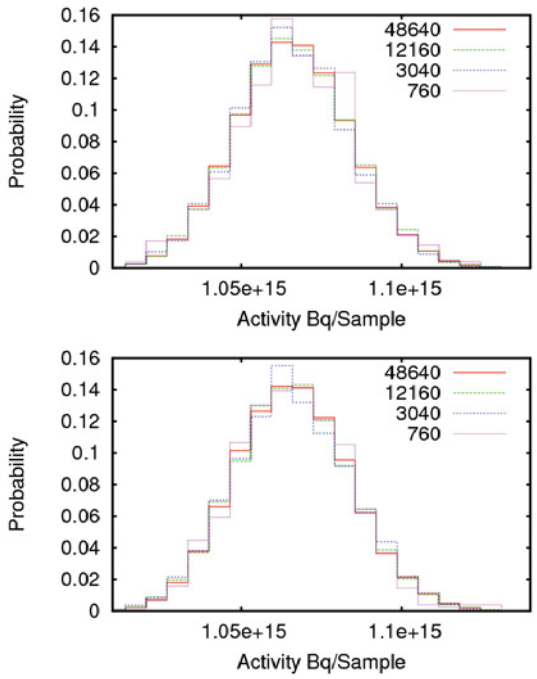

Figure 1: Analysis of the Alloy test case results, studying convergence with number of Monte Carlo samples, listed in the diagram. At the top is the full (F) case, below is the pathways reduced (R) case.

Table 3: Gaussian fits to distributions of activity produced by Monte Carlo sampling of reaction coefficients. The distribution means μ, standard deviations σ and normalisations M_f are each measured in Bq/sample, whereas the statistical errors are given as percentages. Lines labelled F contain results for full FISPACT-II computations, whereas those labelled R are pathways reduced. Cases where fitting was apparently impossible have been omitted.

The Gaussian distribution is defined as $f_G(x) = \frac{M_f}{\sigma\sqrt{2\pi}} \exp -\frac{(x-\mu)^2}{2\sigma^2}$.

	μ	% error	σ	% error	M_f	% error
Alloy						
F	1.06252×10^{15}	0.01078	1.78925×10^{13}	0.6413	6.49737×10^{12}	0.5542
R	1.06241×10^{15}	0.01255	1.78981×10^{13}	0.7463	6.50396×10^{12}	0.6449
Alloy+c						
F	2.62494×10^{13}	0.1519	1.30939×10^{12}	3.089	4.40189×10^{11}	2.649
N	2.63444×10^{13}	0.1486	1.32886×10^{12}	2.984	4.39769×10^{11}	2.562
Fe						
F	1.38941×10^{14}	0.04246	4.77267×10^{12}	1.234	1.49789×10^{12}	1.069
R	1.38531×10^{14}	0.05591	4.72156×10^{12}	1.636	1.4923×10^{12}	1.419
Fiss						
F	1.11555×10^{14}	-	7.71499×10^{9}	2.153	2.47915×10^{9}	-
R	1.11505×10^{14}	-	7.72509×10^{9}	4.136	2.48529×10^{9}	-
LiMix						
F	2.66037×10^{15}	0.0648	5.18814×10^{13}	3.22	2.40961×10^{13}	2.847
R	2.66×10^{15}	0.06296	5.20237×10^{13}	3.118	2.41618×10^{13}	2.758
WMix						
F	1.5813×10^{16}	0.002322	6.32329×10^{13}	0.5765	2.49504×10^{13}	0.4951
R	1.57981×10^{16}	0.002001	6.38371×10^{13}	0.4915	2.49549×10^{13}	0.4224
Y2O3						
F	2.33223×10^{7}	0.5058	4.37985×10^{6}	2.79	1.2523×10^{6}	2.361
R	2.32559×10^{7}	0.6003	4.23901×10^{6}	3.396	1.24103×10^{6}	2.882

Table 4: Log-normal fits to distributions of activity produced by Monte Carlo sampling of reaction coefficients. The distribution means μ, standard deviations σ and normalisations M_f are each measured in Bq/sample (or its natural logarithm), whereas the statistical errors are given as percentages. Lines labelled F contain results for full FISPACT-II computations, whereas those labelled R are pathways reduced. Cases where fitting was apparently impossible have been omitted.

The log-normal distribution is defined as $f_L(x) = \frac{M_f}{x\sigma\sqrt{2\pi}} \exp -\frac{(\ln x-\mu)^2}{2\sigma^2}$.

	μ	% error	σ	% error	M_f	% error
Alloy						
F	34.5997	0.0004812	0.0168458	0.6265	6.5×10^{12}	0.4761
R	34.5996	0.0005864	0.0168465	0.7651	6.5×10^{12}	0.5818
Alloy+c						
F	30.8999	0.004332	0.0507008	2.509	4.5×10^{11}	2.095
R	30.9033	0.004205	0.0514477	2.4	4.5×10^{11}	2.009
Fe						
F	32.5655	0.001087	0.0344321	0.9055	1.5×10^{12}	0.7256
R	32.5626	0.001647	0.03426	1.376	1.5×10^{12}	1.103
LiMix						
F	35.5174	0.002981	0.0199884	3.526	2.5×10^{13}	2.767
R	35.5186	0.003271	0.0203699	3.848	2.5×10^{13}	3.006
Y2O3						
F	16.9707	0.004738	0.183698	0.4297	1.25×10^{6}	0.3772
R	16.9734	0.007921	0.184567	0.715	1.25262×10^{6}	0.6277
YO2						
F	3.33575	0.213	0.897191	0.856	9.36504	0.7281
R	3.3483	0.1181	0.899322	0.4702	9.39112	0.4023

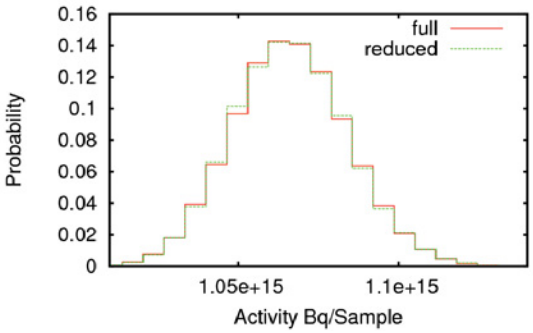

Figure 2: Analysis of the Alloy test case results, showing typical agreement between distributions obtained for the full (F) and (pathways) reduced or R case.

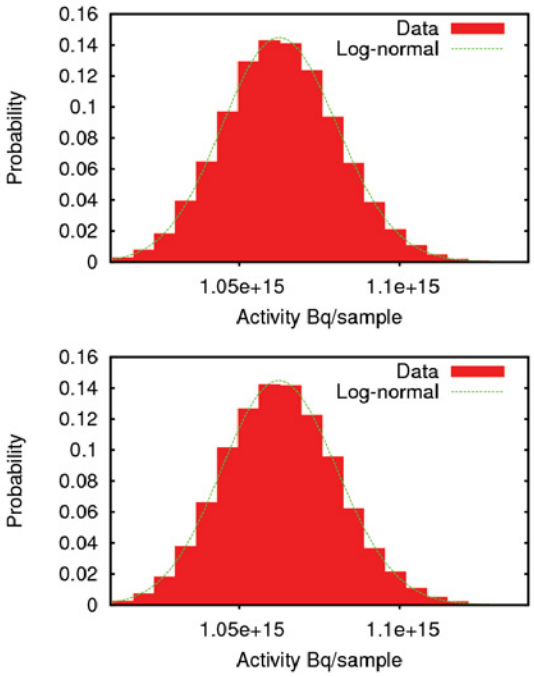

Figure 4: Analysis of the Alloy test case results, showing fits of log-normal functions to the distributions of activity. At the top is the full (F) case, below is the pathways reduced (R) case.

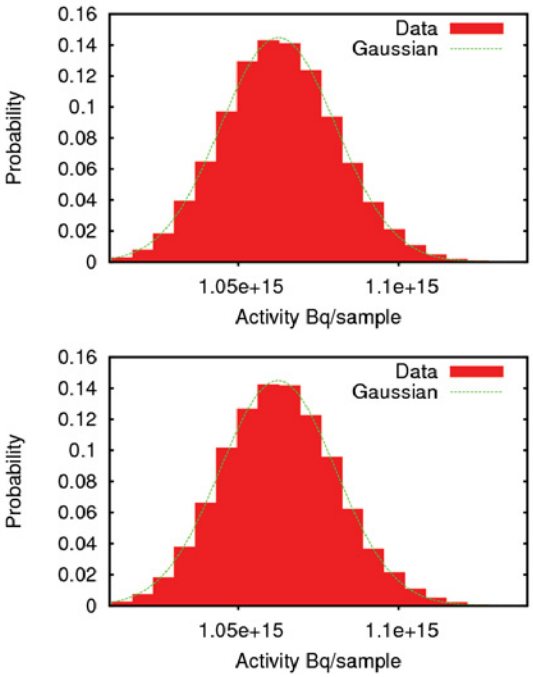

Figure 3: Analysis of the Alloy test case results, showing the fits of Gaussians to the distributions of activity. At the top is the full (F) case, below is the pathways reduced (R) case.

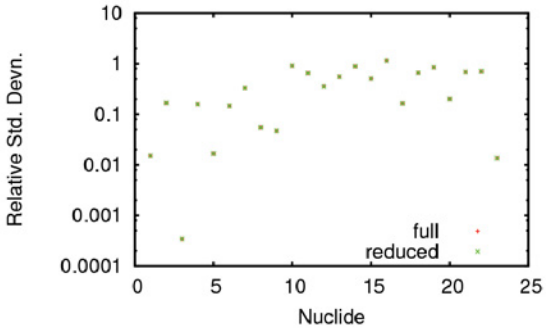

Figure 5: Analysis of the Alloy test case results, showing the typical agreement between relative standard deviations obtained for the full (F) and (pathways) reduced or R cases.

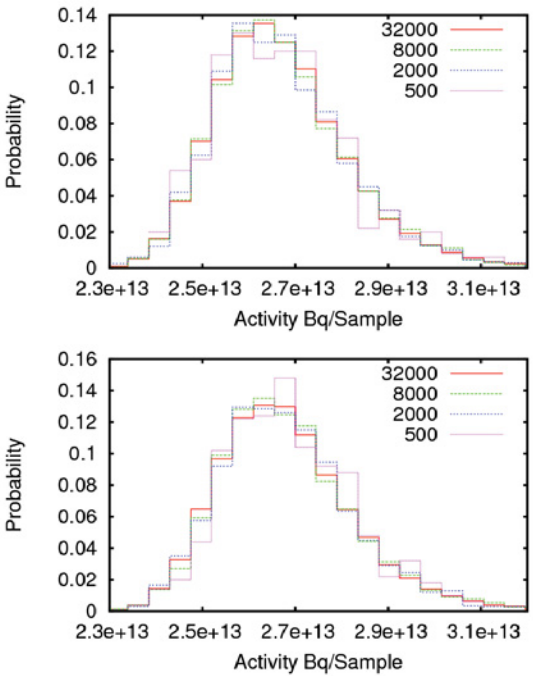

Figure 6: Analysis of the Alloy+c test case results, studying the convergence with number of Monte Carlo samples, listed in the diagram. At the top is the full (F) case, below is the pathways reduced (R) case.

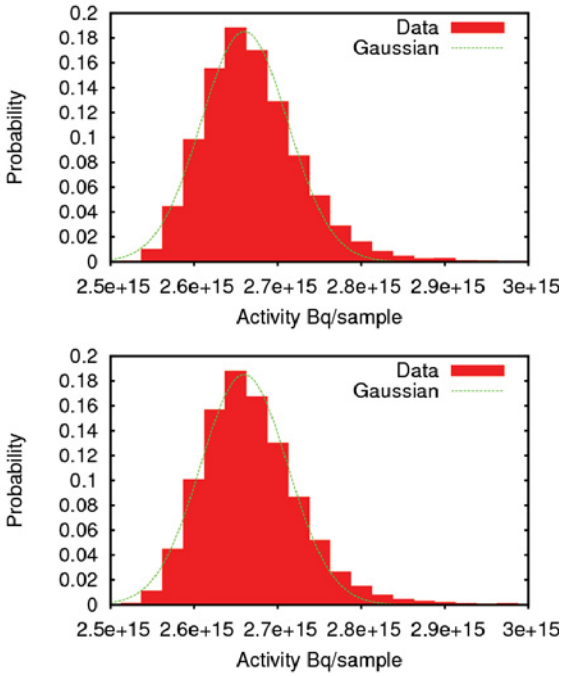

Figure 8: Analysis of the LiMix test case results, showing fits of Gaussians to the distributions of activity. At the top is the full (F) case, below is the pathways reduced (R) case.

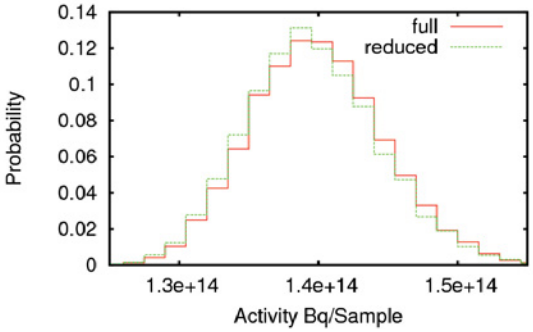

Figure 7: Analysis of the Fe test case results, showing the typical agreement between distributions obtained for the full (F) and (pathways) reduced or R cases.

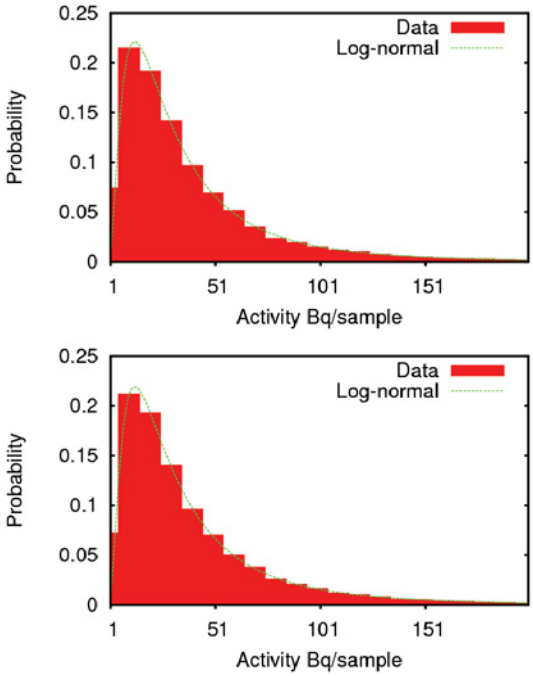

Figure 9: Analysis of the YO2 test case results, showing fits of log-normal functions to the distributions of activity. At the top is the full (F) case, below is the pathways reduced (R) case.

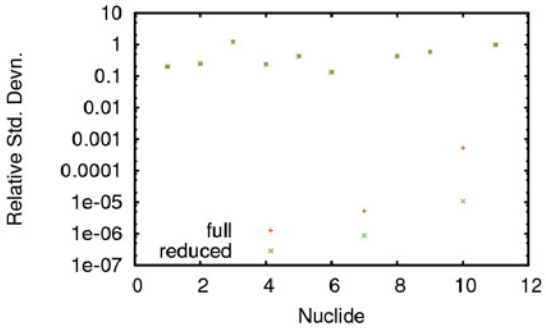

Figure 10: Analysis of the Y2O3 test case results, showing the typical agreement between relative standard deviations obtained for the full (F) and (pathways) reduced or R cases.

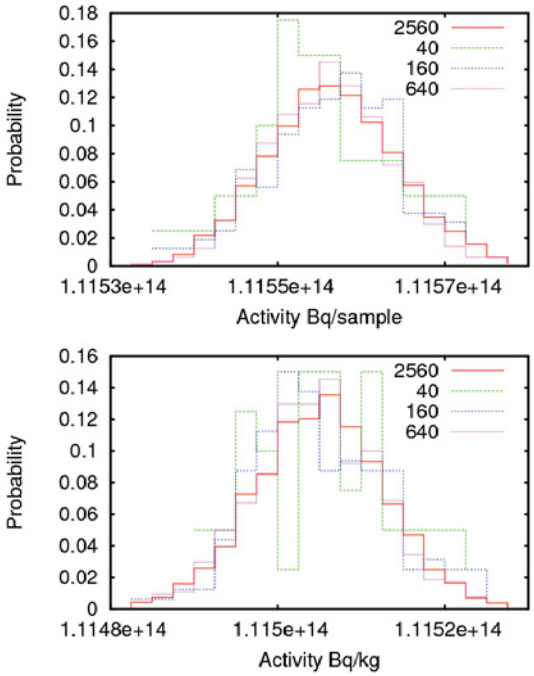

Figure 11: Analysis of the Fiss test case results, studying the convergence with number of Monte Carlo samples, listed in the diagram. At the top is the full (F) case, below is the pathways reduced (R) case.

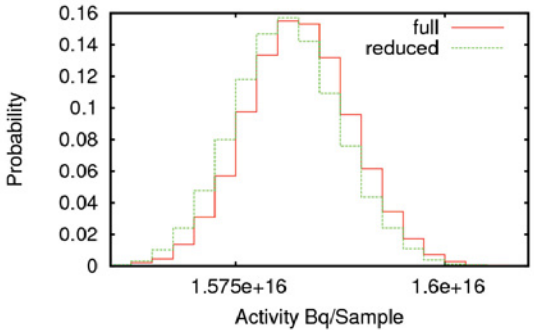

Figure 12: Analysis of the WMix test case results, showing the typical agreement between distributions obtained for the full (F) and (pathways) reduced or R cases.

reduced problems typically execute between 300 to 2 000 times faster. For example, for some problems, it is conceivable that K cannot be reduced below the threshold which would make QMC or other alogrithmic approaches viable, a fact which may now be rapidly discovered. Nonetheless, even in such cases, sensitivity results from rapid, reduced pathways calculations might help to repose or tighten the problem so that sufficiently small K may be found.

Acknowledgment

This work was funded by the RCUK Energy Programme under grant EP/I501045. To obtain further information on the data and models underlying this paper please contact PublicationsManager@ccfe.ac.uk.

References

1) Sublet, J.-C. and Eastwood, J.W. and Morgan, J.G., "The FISPACT-II User Manual," CCFE-R(11)11, CCFE (2013).
2) M. Kalos and P. Whitlock, *Monte Carlo Methods. Vol. 1: basics*, Wiley-Interscience New York, NY, USA (1986).
3) H. Niederreiter, *Random Number Generation and Quasi-Monte Carlo Methods*, Society for Industrial Mathematics (1992).
4) V. Sinescu and P. L'Ecuyer, "Variance bounds and existence results for randomly shifted lattice rules," *Journal of Computational and Applied Mathematics*, **236**, *13*, 3296–3307 (2012).
5) Eastwood, J.W. and Morgan, J.G., "Pathways and uncertainty prediction in Fispact-II," *Proc. Joint International Conference on Supercomputing in Nuclear Applications and Monte Carlo 2013*, 2013, submitted.
6) D. Cacuci and M. Ionescu-Bujor, "A comparative review of sensitivity and uncertainty analysis of large-scale systems. II: Statistical methods," *Nuclear Science and Engineering*, **147**, *3*, 204–217 (2004).
7) F. Campolongo, A. Saltelli, and J. Cariboni, "From screening to quantitative sensitivity analysis. A unified approach," *Computer Physics Communications*, **182**, *4*, 978–988 (2011).
8) J. Eastwood, "Using Graph Theory Methods for Enumerating Pathways," CEM/081203/TN/1, Culham Electromagnetics (2010).
9) T. Williams, C. Kelley, and many others, "Gnuplot 4.2: an interactive plotting program," http://gnuplot.sourceforge.net/, 2009.